

# Brillouin scattering induced transparency and non-reciprocal light storage

Chun-Hua Dong<sup>1,2,\*</sup>, Zhen Shen<sup>1,2</sup>, Chang-Ling Zou<sup>1,2,†</sup>, Yan-Lei Zhang<sup>1,2</sup>, Wei Fu<sup>1,2</sup>, and Guang-Can Guo<sup>1,2</sup>

<sup>1</sup>Key Laboratory of Quantum Information, University of Science and Technology of China, Hefei 230026, P. R. China. and

<sup>2</sup>Synergetic Innovation Center of Quantum Information and Quantum Physics, University of Science and Technology of China, Hefei, Anhui 230026, P. R. China.

Stimulated Brillouin scattering (SBS) is a very fundamental interaction between light and travelling acoustic waves [1, 2], which is mainly attributed to the electrostriction and photoelastic effects with the interaction strength being orders of magnitude larger than other nonlinearities. Although various photonic applications for all-optical light controlling based on SBS have been achieved in optical fiber and waveguides [3–6], the coherent light-acoustic interaction remains a challenge. Here, we experimentally demonstrated the Brillouin scattering induced transparency (BSIT) in a high quality optical microresonator. Benefited from the triple-resonance in the whispering gallery cavity, the photon-phonon interaction is enhanced, and enables the light storage to the phonon, which has lifetime up to 10  $\mu$ s. In addition, due to the phase matching condition, the stored circulating acoustic phonon can only interact with certain direction light, which leads to non-reciprocal light storage and retrieval. Our work paves the way towards the low power consumption integrated all-optical switching, isolator and circulator, as well as quantum memory.

Stimulated Brillouin Scattering (SBS) in fiber and waveguide has stimulated various photonic applications in past decades [1, 2], such as light storage [3], slow light [4], laser [5] and optical isolator [6]. Recently, great progresses have been achieved by incorporating the SBS into photonic integrated chips. On the one hand, the experimentally demonstrated on-chip SBS [7], where the tightly confinement of fields in the compact integrated devices, has greatly enhanced the SBS interaction [8]. And new physics at nanoscale that giant enhancement of SBS due to radiation pressures or boundary-induced nonlinearities have also been revealed [8, 9]. On the other hand, the SBS have been demonstrated in whispering gallery microresonators, such as silica microsphere [10] and disk [11], crystalline cylinders [12]. Around the equator of the microresonators, optical and acoustic waves circulating along the surface, form ultrahigh quality factor whispering gallery modes (WGMs). Benefited from the high quality (Q) factor and small mode volume, the SBS is greatly enhanced when pump, Stocks/anti-Stocks and acoustic modes are triply on-resonance. This opens new

opportunities for coherent light-acoustic interactions in integrated chips. In last few years, low threshold Brillouin lasers [12], Brillouin optomechanics [13, 14] and Brillouin cooling [15, 16] have been reported in such triple-resonance WGMs.

In this study, we demonstrated coherent Brillouin scattering induced transparency (BSIT) and non-reciprocal light storage in a silica microsphere resonator. Placing a strong optical control field on the low frequency optical WGM, coherent interaction between acoustic and the other optical WGMs induces a transparency window for the probe light, which is on resonance with another WGM. Different from the optomechanically induced transparency (OMIT) that have been observed in a variety of optomechanic systems [17, 18], two optical modes are on resonance with forward Brillouin acoustic mode in BSIT. Based on the BSIT, a number of remarkable coherent or quantum optical phenomena are possible, such as light storage, dark modes and frequency conversion [19–21]. Especially, we have demonstrated the non-reciprocal light storage by the SBS, which is potential for quantum memory. These results make the SBS be great candidate for classical and quantum information processing in photonic integrated circuits.

In a silica microsphere resonator, there are optical and acoustic whispering gallery modes (WGMs), which propagate along the surface [Fig. 1(a)]. Both optical and acoustic WGMs are quantized by the orbit angular momentum  $m$ . When the acoustic WGM ( $a$ ) and two optical WGMs ( $c$  and  $d$ ) satisfy the energy and momentum conservations that  $\omega_a = \omega_d - \omega_c$  and  $m_a = m_d - m_c$ , photons can be scattered between the optical resonances through Brillouin scattering [13]. In this work, we focus on the forward SBS that  $m_c$  and  $m_d$  are with the same sign, and both optical modes are coupling to tapered fiber, as depicted in Figs. 1(a) and 1(c). As schematically shown in Fig. 1(b), SBS of the pumping on the optical mode with lower frequency ( $\omega_c$ ) leads to phonon absorption and anti-Stocks photon generation ( $\omega_c + \omega_a$ ), while the Stocks process is inhibited. In reverse, the probe light around  $\omega_d$  generates phonons and Stocks photons.

We firstly study the SBS by only pump laser around  $\omega_c$ . We choose a silica microsphere with radius of 98  $\mu$ m, and find a triple-resonance around wavelength 1562 nm. The scattered anti-Stocks light is detected by measuring the beating signal between the pump and scattered light, and the corresponding spectral line is monitored by an electrical spectrum analyzer, as shown in Fig. 1(d). The Lorentz-shaped peak indicates an acoustic WGM with frequency  $\omega_a/2\pi = 42.3$  MHz and linewidth  $\gamma_a/2\pi = 4$

\*Electronic address: chunhua@ustc.edu.cn

†Electronic address: clzou321@ustc.edu.cn

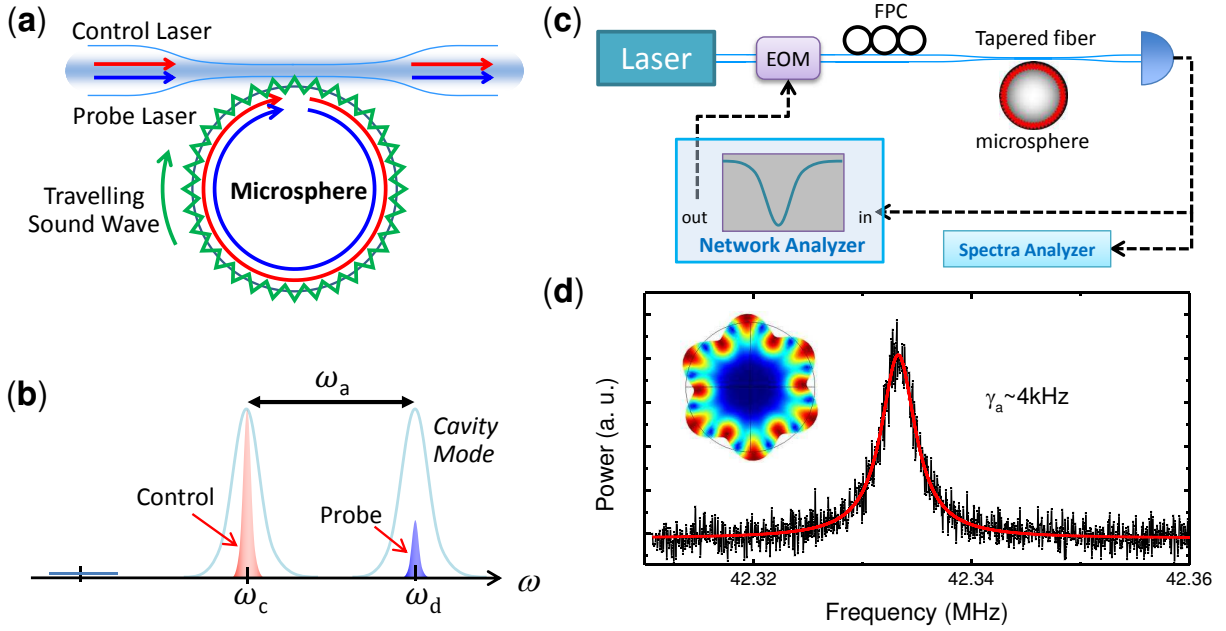


FIG. 1: **Experimental setup of Brillouin scattering in silica microsphere.** (a) Schematic illustration of the light-acoustic interaction in microsphere. The optical modes of the microsphere are excited by the pump and probe lasers through the tapered fiber, and interacting with traveling sound wave through the forward Brillouin scattering. (b) Energy diagram of the coherent photon-phonon interaction: pump light is near-resonance with the lower frequency mode, and the anti-Stocks light as probe light is on-resonance with another cavity mode while Stocks process is suppressed. (c) The experimental setup. EOM: electro-optical modulator; FPC: Fiber polarization controller. (d) The experimental data shows the typical mechanical mode at 42.3 MHz in the microsphere when only pump laser is fixed on-resonance with  $\omega_c$ , the oscillation is due to the beating between pump and scattered anti-Stocks light. Inset: Simulation result of the Brillouin scattering mode with  $m_a = 6$  and frequency is 42.2 MHz.

kHz ( $Q \approx 10600$ ). The acoustic WGM is also verified by measuring the Stocks scattering [see Fig. S1]. From the numerical simulation by finite element method, the orbit angular momentum of acoustic WGM is identified by  $m_a = 6$  [Inset of Fig.1(d)].

Considering the interaction of forward SBS in the triple-resonance system, the Hamiltonian can be written as

$$H = \omega_a a^\dagger a + \omega_c c^\dagger c + \omega_d d^\dagger d + g(a^\dagger c^\dagger d + a c d^\dagger), \quad (1)$$

where  $a$ ,  $c$ ,  $d$  are Boson operators of acoustic and optical modes [Fig. 1(b)]. We should note that the vacuum SBS strength  $g$  is nonzero only when the three modes are traveling along the same direction. The energy diagram of the system is illustrated schematically in Fig. 2(a), where energy levels are described by phonon and photon Fock state  $|n_a, n_c, n_d\rangle$ , where  $n_{a(c,d)}$  is phonon (photon) number. The SBS is a parametric process which induces the transitions between  $|n_a, n_c, n_d + 1\rangle$  and  $|n_a + 1, n_c + 1, n_d\rangle$ , leads to Boson annihilation and creation of all three modes. The pump and probe lights induce the transitions that change the photon number of  $c$  or  $d$  mode, described by the Hamiltonian  $H_p = i\sqrt{\kappa_{c,1}}\epsilon_l(c^\dagger e^{-i\omega_l t} - c e^{i\omega_l t}) + i\sqrt{\kappa_{d,1}}\epsilon_p(d^\dagger e^{-i\omega_p t} - d e^{i\omega_p t})$ . Here,  $\epsilon_l$  is strong control laser with frequency  $\omega_l$  driving on optical mode  $c$ , and  $\epsilon_p$  is weak probe light with

frequency  $\omega_p$  coupling to mode  $d$  [Fig. 1(b)].  $\kappa_{c,1}$  and  $\kappa_{d,1}$  are the coupling strength of modes  $c$  and  $d$  to the waveguide, respectively.

The vacuum SBS strength  $g$  is very weak compared to photon dissipation rate  $\kappa_{c,d}$ , thus the  $c$  mode is pumped to enhance the interaction between phonon  $a$  and photon  $d$ , just as people usually do in the difference frequency generation or sum frequency processes in nonlinear optical  $\chi^{(2)}$  processes. For the mean field  $\langle c \rangle = \sqrt{N_c} = \left| \frac{\sqrt{\kappa_{c,1}}\epsilon_l}{-i\Delta_c - \kappa_c} \right|$  with  $\Delta_c = \omega_c - \omega_l$ , the total Hamiltonian is simplified in rotating frame as

$$H = -\delta a^\dagger a - (\delta + \Delta) d^\dagger d + g\sqrt{N_c}(a^\dagger d + a d^\dagger) + i\sqrt{\kappa_{d,1}}\epsilon_p(d^\dagger - d), \quad (2)$$

where detuning  $\delta = \omega_p - \omega_l - \omega_a$  and  $\Delta = \omega_a + \omega_l - \omega_d$ . For a probe laser is near-resonance with  $|n_a, n_d\rangle$  and  $|n_a, n_d + 1\rangle$ , the model assembles the well-known electromagnetic induced transparency in  $\Lambda$ -type atom. The similar steady state intracavity power spectrum is solved as

$$I_d(\delta) \propto \left| \frac{\kappa_{d,1}}{i(\delta + \Delta) - \kappa_d/2 + \frac{g^2 N_c}{i\delta - \gamma_a/2}} \right|^2. \quad (3)$$

The intracavity power of optical mode  $d$  is modified by the coherent photon-phonon interaction, giving rise to

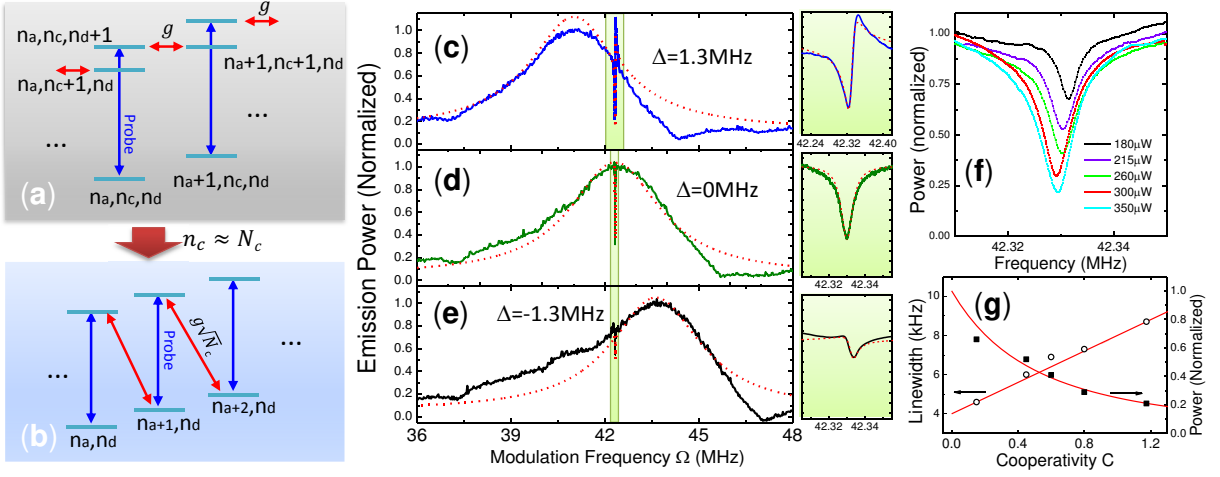


FIG. 2: **Mechanism and observation of BSIT.** (a-b) The energy diagram of the triple-resonance in the whispering-gallery cavity. (c-e) Experimentally observed normalized heterodyne traces when the probe frequency is scanned by sweeping the phase modulator frequency  $\Omega$  for different values of control beam detuning  $\Delta = -1.3, 0, 1.3$  MHz. Whereas the center of the response of the bare optical cavity shifts correspondingly, the sharp dip characteristic of BSIT occurs always for  $\delta\omega = 0$ . The input power of the control beam launched to the cavity is  $0.3 \mu\text{W}$  during the measurements. The insets show the spectral response in the relevant anti-stokes resonance, with an expanded frequency scale. The short dash lines are the calculation results with the parameters  $k_d/2\pi, \gamma_a/2\pi, G/2\pi = 3.5, 0.004, (0.14, 0.05, 0.03)$  MHz. (f) The emission power from the WGM near the anti-stokes resonance for four different powers in the control beam from  $0.18$  mW up to  $0.35$  mW. The lines are the calculated results. (g) The spectral linewidth of the BSIT dip and the emission power from the WGM as a function of the mechanical cooperativity, derived from (f). The solid lines in (g) show the theoretically expected values for the linewidth and emission power.

changes of transmission when  $\frac{g^2 N_c}{i\delta - \gamma_a/2}$  is comparable to  $\kappa_d$ . It's convenient to introduce the cooperativity factor  $C = \frac{4g^2 N}{\gamma_a \kappa_d}$  to evaluate the coherent interaction strength, and  $C \gg 1$  is preferred for high fidelity information processing.

To verify the BSIT in our system, we probe the cavity transmission spectrum in the presence of a control beam. The probe light is generated from the modulated control laser by EOM, which is modulated at frequency  $\Omega$ . The measured total heterodyne signal with the modulation frequency  $\Omega$  using a network analyzer allows extracting intracavity power, which is directly related to the probe transmission [Supplementary Information]. In Figs. 2(c)-(e), we investigate the dependence of the transparency window on the detuning  $\Delta$  by adjusting  $\omega_l$  with fixed pumping power  $P = 300 \mu\text{W}$ . The shift of transparency window follows the triple resonance condition when  $\delta = 0$ , and the asymmetric Fano-type lineshapes are in good agreement with theoretical model [Eq. (3)]. We estimate the  $C = 5.9, 0.75, 0.27$  for  $\Delta = 1.3, 0, -1.3$  MHz. The strongest coupling rate isn't at the detuning  $\Delta = 0$ , because of the triple-resonance condition is not exactly satisfied as  $\omega_d - \omega_c - \omega_a \approx 1.3$  MHz. Further studies of BSIT dip at  $\Delta = 0$  are shown by Fig. 3(f), for pump power varying from  $180 \mu\text{W}$  to  $350 \mu\text{W}$ . Dips of increasing depth and width are observed, which can be fitted by a simple Lorentz function. From Eq. 3, the expected linewidth is linearly increasing with  $C$  relationship as  $(1+C)\gamma_a$ , and the minimum intracavity power of

the BSIT is given by  $\frac{1}{(1+C)^2}$ . However, we find the  $C$  is not proportional to the input power, due to the thermal effect that changed the triple-resonance condition.

Owing to the coherent SBS interaction, the coherent conversion between phonon and acoustic phonon could be used for light storage. Especially, the phase matching conditions of the triple-resonances breaks the reversal of light propagation. Different from previously studied radiation and gradient forces driven optomechanics, where mechanical vibrations could couple to a variety of optical modes, the Brillouin scattering is only possible for specific mode satisfied energy and momentum conservation conditions. For example, the input clockwise (CW) pump laser only permits the interaction between CW acoustic phonon and photon, while the counter-clockwise (CCW) probe light or acoustic wave is not affected by SBS. To verify this non-reciprocity, we have studied the light storage for CW or CCW signal input with fixed CW pump light, as shown in Fig. 3(a). As evident from the plot, the CW propagating signal (Black line) is stored and retrieved after  $3 \mu\text{s}$ . During the writing pulse, the measured signal is decreased by the time because of the dynamical behavior of BSIT, and similar phenomenon has been reported of breathing mode in Ref.[22]. After the writing pulse, the decay time of the emission power is calculated with  $14 \mu\text{s}$  (Green dashed line in Fig. 3(a)), which is corresponding to the mechanical linewidth of  $15$  kHz. For the CCW launched signal (Red line), there is no light retrieval during the reading pulse. It's worth noting that

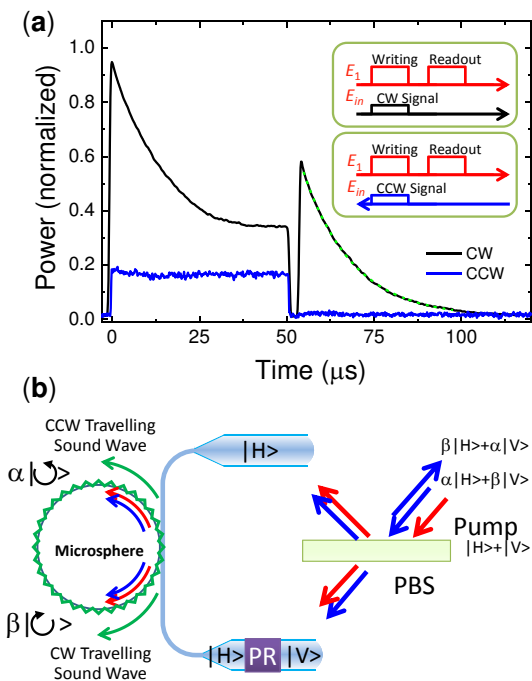


FIG. 3: **Non-reciprocal light storage and proposed quantum memory.** (a) The light storage and retrieval from different input direction. Inset: the pulse sequence for writing, readout and signal. (b) Schematics of the single bit quantum memory based on the circulating acoustic phonons. PBS: polarization beam splitter; PR: polarization rotator.

the flat signal in writing pulse is derived from the reflected signal at the end face of the circulator.

In the previous sections, we have provided experimental evidence of coherent and non-reciprocal photon-phonon conversion for the SBS in silica microsphere. Therefore, the degenerated clockwise and counter-clockwise acoustic modes can be written and read out coherently and independently. Benefit from these, we proposed a quantum memory of polarization encoded photon state. As depicted in Fig. 3(b), the horizontal (vertical) polarized input photon state can couple to CW and CCW optical modes, store as the CW and CCW acoustic waves and read out, separately. Ideally, the input state as a superposition of polarization state  $\alpha|H\rangle + \beta|V\rangle$  can be stored as superposition of circulating acoustic state  $\alpha|\dot{\circ}\rangle + \beta|\dot{\circ}\rangle$ . As a reversal of the storage, the states are read out by converting to the photon state  $\alpha|V\rangle + \beta|H\rangle$  after tens of microseconds.

The Brillouin scattering in the whispering gallery microresonators is advanced in several aspects. (a) The Brillouin scattering enables the optical coupling to acoustic wave with frequency range from few MHz to 11 GHz, providing a diversified platform for coherent light-matter interaction. (b) The triple-resonance configure can en-

hance the SBS, thus reduce the power consumptions. (c) The traveling wave properties bring the light non-reciprocity, thus potential for all-optical integrated non-reciprocal devices, such as isolator and circulator. Our studies pave the way towards the strong coupling between photon and acoustic phonon, and encourage further investigations of the non-reciprocity and memory at quantum level.

*Note:* During the preparation of this manuscript, a similar work has reported in the Conference on Lasers & Electro-optics [23].

## Method

Silica microspheres are fabricated by melting the tapered fiber with a CO<sub>2</sub> laser. Optical WGMs in the microsphere are excited through evanescent field of a tapered optical fiber with a tunable narrow linewidth (< 300 kHz) external-cavity laser at the 1550 nm band. The experiment setup is schematically illustrated in Fig. 1(c). All experiments are performed at room temperature and atmospheric pressure.

The coupling strength between the tapered fiber and optical WGMs could be adjusted by changing the air gap between them, which was controlled by a high resolution translation stage. The output light is detected by a low-noise photo-receiver, which was connected to a digital oscilloscope to measure the transmission spectra or a spectra analyzer to find the Brillouin scattering modes. For the BSIT experiment, the laser beam is modulated by the EOM to generate sideband as the probe light. A network analyzer is used to generate the modulation signal of EOM, and also measure the spectrum density of beating signal, which corresponding to the emission power from WGMs.

The measurement of non-reciprocity is carried out by two separated AOMs, as shown in Fig. S2. A Brillouin mode with  $\omega_a = 152.7$  MHz is chosen to match the working frequency of the acousto-optic modulators (AOM 1 and 2). The writing and reading pulse array is generated by AOM 1, where a laser beam is frequency shifted by  $-80$  MHz. The signal pulse is obtained by AOM 2, which is synchronization with the writing pulse but the frequency is shifted by  $+72.7$  MHz. The power of writing and reading pulses are 1 mW and the power of signal is 20 nW. The duration of writing and reading pulse are 50  $\mu$ s and 80  $\mu$ s, respectively. The two pulses are separated by 3  $\mu$ s as storage time. The forward and backward signal pulse are coupled into the fiber separately. The power of emitted light is measured from the spectra analyzer with gate detection mode, and the resolution bandwidth is 10 MHz.

[1] A. Kobayakov, M. Sauer, and D. Chowdhury, "Stimulated Brillouin scattering in optical fibers," Adv. Opt. Photon-

- [2] B. Eggleton, C. Poulton, and R. Pant, “Inducing and harnessing stimulated Brillouin scattering in photonic integrated circuits,” *Adv. Opt. Photonics* **6**, 536–587 (2013).
- [3] Z. Zhu, D. J. Gauthier, and R. W. Boyd, “Stored light in an optical fiber via stimulated Brillouin scattering,” *Science* **318**, 1748–50 (2007).
- [4] Y. Okawachi, M. S. Bigelow, J. E. Sharping, Z. M. Zhu, A. Schweinsberg, D. J. Gauthier, R. W. Boyd, and A. L. Gaeta, “Tunable all-optical delays via Brillouin slow light in an optical fiber,” *Phys. Rev. Lett.* **94**, 153902 (2005).
- [5] K. S. Abedin, P. S. Westbrook, J. W. Nicholson, J. Porque, T. Kremp, and X. Liu, “Single-frequency Brillouin distributed feedback fiber laser,” *Opt. Lett.* **37**, 605–607 (2012).
- [6] X. Huang and S. Fan, “Complete All-Optical Silica Fiber Isolator via Stimulated Brillouin Scattering,” *J. Light. Technol.* **29**, 2267–2275 (2011).
- [7] R. Pant, C. G. Poulton, D. Y. Choi, H. McFarlane, S. Hile, E. Li, L. Thevenaz, B. Luther-Davies, S. J. Madden, and B. J. Eggleton, “On-chip stimulated Brillouin scattering,” *Opt. Express* **19**, 8285–8290 (2011).
- [8] H. Shin, W. Qiu, R. Jarecki, J. a Cox, R. H. Olsson, A. Starbuck, Z. Wang, and P. T. Rakich, “Tailorable stimulated Brillouin scattering in nanoscale silicon waveguides,” *Nat. Commun.* **4**, 1944 (2013).
- [9] P. T. Rakich, C. Reinke, R. Camacho, P. Davids, and Z. Wang, “Giant Enhancement of Stimulated Brillouin Scattering in the Subwavelength Limit,” *Phys. Rev. X* **2**, 011008 (2012).
- [10] M. Tomes and T. Carmon, “Photonic Micro-Electromechanical Systems Vibrating at X-band (11-GHz) Rates,” *Phys. Rev. Lett.* **102**, 113601 (2009).
- [11] J. Li, H. Lee, and K. J. Vahala, “Microwave synthesizer using an on-chip Brillouin oscillator,” *Nat. Commun.* **4**, 2097 (2013).
- [12] I. S. Grudin, A. B. Matsko, and L. Maleki, “Brillouin Lasing with a CaF<sub>2</sub> Whispering Gallery Mode Resonator,” *Phys. Rev. Lett.* **102**, 043902 (2009).
- [13] G. Bahl, J. Zehnpfennig, M. Tomes, and T. Carmon, “Stimulated optomechanical excitation of surface acoustic waves in a microdevice,” *Nat. Commun.* **2**, 403 (2011).
- [14] G. Bahl, K. H. Kim, W. Lee, J. Liu, X. Fan, and T. Carmon, “Brillouin cavity optomechanics with microfluidic devices,” *Nat. Commun.* **4**, 1994 (2013).
- [15] G. Bahl, M. Tomes, F. Marquardt, and T. Carmon, “Observation of spontaneous Brillouin cooling,” *Nat. Phys.* **8**, 203–207 (2012).
- [16] M. Tomes, F. Marquardt, G. Bahl, and T. Carmon, “Quantum-mechanical theory of optomechanical Brillouin cooling,” *Phys. Rev. A* **84**, 063806 (2011).
- [17] S. Weis, R. Rivière, S. Deléglise, E. Gavartin, O. Arcizet, A. Schliesser, and T. J. Kippenberg, “Optomechanically induced transparency,” *Science* **330**, 1520–3 (2010).
- [18] H. Safavi-Naeini, T. P. Mayer Alegre, J. Chan, M. Eichenfield, M. Winger, Q. Lin, J. T. Hill, D. E. Chang, and O. Painter, “Electromagnetically induced transparency and slow light with optomechanics,” *Nature* **472**, 69–73 (2011).
- [19] C. Dong, V. Fiore, M. C. Kuzyk, and H. Wang, “Optomechanical dark mode,” *Science* **338**, 1609–13 (2012).
- [20] J. T. Hill, A. H. Safavi-Naeini, J. Chan, and O. Painter, “Coherent optical wavelength conversion via cavity optomechanics,” *Nat. Commun.* **3**, 1196 (2012).
- [21] V. Fiore, Y. Yang, M. C. Kuzyk, R. Barbour, L. Tian, and H. Wang, “Storing Optical Information as a Mechanical Excitation in a Silica Optomechanical Resonator,” *Phys. Rev. Lett.* **107**, 133601 (2011).
- [22] C. Dong, V. Fiore, M. C. Kuzyk, and H. Wang, “Transient optomechanically induced transparency in a silica microsphere,” *Phys. Rev. A* **87**, 055802 (2013).
- [23] J. Kim, M. Kuzyk, K. Han, H. Wang, and G. Bahl, “Observation of Brillouin Scattering Induced Transparency in a Silica Microsphere Resonator,” in *CLEO: 2014, OSA Technical Digest (online)* (Optical Society of America, 2014), paper SF2M.5.

### Acknowledgment

C.H.D. and Z.S. contribute equally to this work. The work was supported by the National Basic Research Program of China (Grant No.2011CB921200), the Knowledge Innovation Project of Chinese Academy of Sciences (Grant No.60921091), the National Natural Science Foundation of China (Grant No.61308079), the Fundamental Research Funds for the Central Universities.

### Author Contribution

All authors contributed extensively to the work presented in this paper. C.H.D. and Z.S. prepared microsphere and carried out experiment measurements. C.L.Z., Y.L.Z. and W.F. provided theoretical support and analysis. C.L.Z. and C.H.D. wrote the manuscript. C.H.D., C.L.Z. and G.C.G. supervised the project.

### Competing Interests

The authors declare that they have no competing financial interests.

### Correspondence

Correspondence and requests for materials should be addressed to Chunhua Dong (chunhua@ustc.edu.cn) and Chang-Ling Zou (clzou321@ustc.edu.cn).